Oncogenic K-Ras segregates at spatially distinct plasma membrane signaling platforms according to its phosphorylation status

Carles Barceló[1], Noelia Paco[1], Alison J. Beckett[2], Blanca Alvarez-Moya[1], Eduard Garrido[1], Mariona Gelabert[1], Francesc Tebar[1], Montserrat Jaumot[1], Ian Prior[2] and Neus Agell[1*]

[1]Departament de Biologia Cel·lular, Immunologia i Neurociències, Institut d'Investigacions Biomèdiques August Pi i Sunyer (IDIBAPS), Facultat de Medicina. Universitat de Barcelona, C/ Casanova 143, 08036 Barcelona, Spain

[2] Physiological Laboratory, Department of Molecular and Cellular Physiology, Institute of Translational Research, University of Liverpool, Crown St., Liverpool L69 3BX, UK

Running title: K-Ras domains by phosphorylation

Keywords: K-Ras, nanoclustres, Raf, PI3K, PKC, phosphorylation

*Author for correspondence (neusagell@ub.edu)

JCS Advance Online Article. Posted on 13 August 2013

Summary

Activating mutations in the K-Ras small GTPase are extensively found in human tumors. Although these mutations induced the generation of a constitutively GTP-loaded, active form of K-Ras, phosphorylation at Ser181 within the C-terminal hypervariable region is able to modulate oncogenic K-Ras function without affecting the *in vitro* affinity for its effector Raf-1. In striking contrast, K-Ras phosphorylated at Ser181 showed an increased interaction with active form of Raf-1 and for PI3K (p110α) in cells. As most phosphorylated K-Ras is located at the plasma membrane, differential localization within this membrane according to the phosphorylation status was explored. Plasma membrane density gradient fractionation in the absence of detergents showed segregation of phosphomimetic and non-phosphorylatable K-Ras mutants (Ser181D and Ser181A, respectively). Moreover, immuno-electron-microscopy-statistics analysis showed that both phosphorylation mutants form distinct non-overlapping nanoclusters. Finally, promotion or inhibition of oncogenic K-Ras phosphorylation by PKC increased its co-clustering with the phosphomimetic or the non-phosphorylatable mutant, respectively. Most interestingly, PI3K (p110α) was found in phosphorylated and excluded in non-phosphorylated K-Ras nanoclusters. In conclusion, our data provide for the first time evidences that phosphorylation of oncogenic K-Ras by PKC induces segregation of K-Ras in spatially distinct nanoclusters at the plasma membrane which in turn would favor Raf-1 and PI3K activation.

INTRODUCTION

Somatic activating Ras mutations are detected in about 15 to 20% of all human malignancies highlighting the importance of Ras GTPase-mediated signaling pathways in oncogenesis. These mutations, which give rise to a protein that is defective for GTP hydrolysis and, therefore, remains constitutively active in a GTP-bound form, have been detected in each of the three closely related human Ras genes (Hras, Nras, and Kras). However, the vast majority of mutations detected in human cancers arise in the K-Ras gene (Prior et al., 2012;Pylayeva-Gupta et al., 2011;Schubbert et al., 2007).

H- and N-Ras achieve high-affinity hydrophobic membrane binding mainly through lipid modifications. In contrast, K-Ras has, adjacent of the farnesylated cysteine, a stretch of lysine residues- known as the polybasic domain - which promotes an electrostatic interaction with the negatively-charged phospholipids (Hancock et al., 1989;Silvius, 2002) confining K-Ras almost entirely to non-raft plasma membrane microdomains (Prior et al., 2001)

The different membrane anchors interact with lipids and proteins of the plasma membrane and together with the hypervariable region (HVR), drive the Ras isoforms into spatially and structurally distinct nanodomains, each one containing a cluster of molecules (nanocluster) (Abankwa et al., 2008;Hancock and Parton, 2005). Importantly, the nanodomains occupied by the three isoforms of Ras do not show any overlap. Interestingly, not only are the different Ras isoforms laterally segregated, but inactive GDP-loaded Ras occupies nanodomains that are spatially distinct from those occupied by the active GTP-loaded form, indicating that the globular domain of the protein also regulates the interaction with the distinct membrane nanodomains. The formation of these nanoclusters is essential for the mitogen-activated protein kinase (MAPK) activation as they constitute the exclusive sites for Raf-1 recruitment and ERK activation in the plasma membrane (Kholodenko et al., 2010;Plowman et al., 2005;Tian et al., 2007)

As electrostatic interactions control the membrane interaction process for K-Ras, membrane affinity can be modulated by changes in the overall charge of the polybasic domain via Ser181 phosphorylation (Ahearn et al., 2011;Ballester et al., 1987;Bivona et al., 2006;Plowman et al., 2008). In a recent work we demonstrated that Ser181-

phosphorylation regulates both wild-type and oncogenic K-Ras functions. Focus formation capacity, mobility and apoptosis resistance upon adriamycin treatment of cells expressing oncogenic non-phosphorylatable K-Ras were highly compromised, correlating with a decreased activation of main downstream effectors ERK and AKT. Therefore, in our model, K-Ras phosphorylation is essential to ensure a proper activation of ERK and AKT pathways with an important functional relevance (Alvarez-Moya et al., 2010;Alvarez-Moya et al., 2011).

Understanding how phosphorylation modulates oncogenic K-Ras activity is of outstanding interest to design new therapeutic strategies against human carcinomas with oncogenic K-Ras mutations. Here we show, using both, cell fractionation and immuno-electron microscopy techniques, a segregation of oncogenic K-Ras at the plasma membrane according to its phosphorylation status with a potentials impact in effectors activation. We propose that this differential localization can be responsible for the distinct functionality of phosphorylated versus non-phosphorylated K-Ras.

RESULTS AND DISCUSSION

Oncogenic K-Ras phosphorylation at Ser181 favors interaction with active Raf-1 and PI3K catalytic subunit.

We previously showed that phosphorylation of oncogenic K-RasG12V (always GTP-loaded) at Ser181 was positively modulating ERK and AKT activation, especially under stress conditions. However, the *in vitro* affinity between oncogenic K-RasG12V and Raf-1 was not affected by this post-translational modification of K-Ras (Alvarez-Moya et al., 2010), and consequently, it could not explain the differences in ERK activation. Similarly, and in agreement with (Plowman et al., 2008), FRET analysis did not show an increase in the association of phosphomimetic oncogenic K-Ras (Ser181 mutated to Asp, named K-RasG12V-S181D) with Raf-1 compared to the non-phosphorylatable oncogenic K-Ras (Ser181 mutated to Ala, hereinafter referred to as K-RasG12V-S181A) (Fig 1A and B). Interestingly, although interaction of Raf-1 with K-Ras was not affected by the phosphorylation status of K-Ras, immunofluorescence analysis showed that a higher proportion of Raf-1 colocalizing with K-RasG12V-S181D was active, as show by Raf-1 phosphorylation at Ser338 (Fig. 1C and D).

Co-immunoprecipitation analysis corroborated these results. While, the amount of Raf-1 co-immunoprecipitated with non-phosphorylatable oncogenic K-Ras or with phosphomimetic K-Ras was not significantly different, K-RasG12V-S181D shows an increased ability to co-immunoprecipitate with active Raf-1 (P-Ser338). Finally, another K-Ras effector, the catalytic subunit of PtdIns-3 kinase (PI3K), p110α, also showed a higher co-immunoprecipitation with K-RasG12V-S181D than with K-RasG12V-S181A (Fig. 1E). Thus, we hypothesize that Ser181 phosphorylation of oncogenic K-Ras favors activation or retention of activated effectors, through a yet undefined mechanism.

Differential fractionation of phosphorylated and not phosphorylated oncogenic K-Ras at the plasma membrane.

The negative charges introduced in the HVR by phosphorylation might modify the plasma membrane affinity of K-Ras and alter its localization (Yeung et al., 2006). In fact, certain groups have reported that phosphomimetic K-Ras is internalized to intracellular membranes such as mitochondria, Golgi apparatus, endoplasmic reticulum or endosomes (Bivona et al., 2006; Fivaz and Meyer, 2005). In contrast we show here

that after simultaneous transfection of both YFP-K-RasG12V-S181A and mCherry-K-RasG12V-S181D in HEK293 cells, both phosphomutants were mainly located at the plasma membrane (Fig. 2A), in agreement with previous observations (Lopez-Alcala et al., 2008;Plowman et al., 2008). We aimed to analyze whether differential localization within the plasma membrane of phosphorylated versus non-phosphorylated K-Ras could be the basis for the observed differential active Raf-1 and PI3K recruitment.

We aimed to test whether Ser181 phosphorylation of K-Ras could induce its segregation into different plasma membrane domains by performing a cell fractionation in a density gradient. K-Ras, in contrast to N- and H-Ras, is mainly localized in disordered non-raft detergent-sensitive plasma membrane domains (Prior et al., 2001). This constitutes a drawback when studying its distribution using the classical cell fractionation procedures. In our study, membranes from HEK293 cells were fractionated into a detergent free method to prevent the disruption of K-Ras domains was used(Macdonald and Pike, 2005), . As cells were co-transfected with the two K-Ras mutants (YFP-K-RasG12V-S181A and mCherry-K-RasG12V-S181D), a single fractionation and a single gel electrophoresis was performed per experiment, avoiding possible variability in gradient generation or gel loading.

The early endosome marker, EEA1, the endoplasmic reticulum marker, Sec61α, and the caveolar lipid raft marker, Caveolin-1, were confined in the higher density fractions, in contrast, Na^+/K^+ ATPase distribution was extended throughout many fractions (Fig. 2B),. Endogenous K-Ras (wild type) was always found between fractions 4 and 6 (Fig. 2B,C,D,E). Furthermore, both exogenous non-oncogenic (wild-type) YFP-K-Ras and mCherry-K-Ras were found mainly in the same fractions as endogenous wild type K-Ras (Fig S1). When analyzing the exogenous co-expressed oncogenic K-Ras phosphomutants, although a more spread distribution of the protein was observed compared to the endogenous K-Ras we reproducibly observed that non-phosphorylatable K-Ras mutant (K-RasG12V-S181A) peaked between fractions 5-7 while the peak of phosphomimetic K-Ras (K-RasG12V-S181D) shifted towards the higher density fractions 8-10 (Fig- 2B,C,D). A prospective tag-artifact in the differential fractionation was dismissed because when the reverse tagged proteins were used (mChery-K-RasG12V-S181A and YFP-K-RasG12V-S181D), differences of fractionation according to the phosphorylation status were maintained (Fig. 2D and Fig. S1). In agreement with data shown in figure 1B, both p110 α and phospho-Ser338-Raf-1 exhibited higher co-fractionation with K-RasG12V-S181D rather than with the non-

phosphorylatable K-Ras (Fig. 2B). This reinforces the concept of a segregated membrane domain for the phospho-S181-K-Ras that constitutes a preferential signaling platform.

We next analyzed the localization of the phosphorylatable oncogenic K-Ras, (K-RasG12V-S181). As shown in Fig. 2E, the majority of K-RasG12V-S181 was found at the beginning of the gradient while a certain amount fractionated together with K-RasG12V-S181D, suggesting that a proportion of K-RasG12V-S181 is phosphorylated under these conditions.

Segregation of phosphorylated and non-phosphorylated oncogenic K-Ras in non-overlapping clusters at the plasma membrane.

In order to further determine the presence of distinct segregated phosho-Ser181-K-Ras nanodomains that ensure preferential signaling platforms, we attempted to analyze the distribution at the nanoscale level of our oncogenic K-Ras phosphomutants. Analysis of gold-labeled protein distribution using a combined immune-EM-statistics approach allows the characterization of K-Ras nanoclusters in otherwise morphologically featureless plasma membrane (Prior et al., 2003). Furthermore it has also been shown that both phosphorylated and non-phosphorylatable K-Ras are able to form such nanoclusters (Plowman et al., 2008). Since our fractionation experiments indicate segregation of phosphorylated and non-phosphorylatable K-Ras and the inner leaflet of the plasma membrane consists of a mosaic of different nanoclusters (Prior et al., 2003), we wanted to directly compare nanocluster distributions of our K-Ras variants. To this end, cells were co-transfected with both oncogenic K-Ras phospho-mutants fused to either YFP or mCherry. Intact 2D sheets of apical plasma membrane were ripped off from adherent cells directly onto electron microscopy grids and immunogold labeled using anti-GFP antibodies conjugated directly to 5 nm gold particles and anti-RFP antibodies directly conjugated to 10 nm gold particles. To estimate the degree of co-clustering between our K-RasG12V species the Ripley's bivariate K-function was used. As a positive control, co-transfection of the same mutant with different tags was performed to assess if co-clustering could be observed. As expected, YFP-K-RasG12V-S181D co-clustered with mCherryK-RasG12V-S181D, thus dismissing the possibility of a tag-effect. In contrast, if cells were co-transfected with YFP-K-RasG12V-S181D and mCherryK-RasG12V-S181A no co-clustering was observed, providing striking evidences that confirm our initial conception of the existence of a spatially segregated

cluster for phospho-K-RasG12V (Fig. 3A,D). In agreement with Plowman et al (Plowman et al., 2008), the analysis of clusters using the Ripley's univariate K-function in the same samples, showed that both non-phosphorylatable K-Ras and phosphomimetic K-Ras were able to form clusters (data not shown).

Protein Kinase C (PKC) can phosphorylate K-Ras *in vitro* (Ballester et al., 1987), and it has been shown *in vivo* that phosphorylation of Ser181 is induced under conditions of PKC activation (PMA) and CaM inhibition (W13) while reduced after treatment with PKC inhibitors (BIM) (Alvarez-Moya et al., 2010). To conclusively demonstrate that Ser181 phosphorylation was regulating the localization of oncogenic K-Ras in different nanoclusters at the plasma membrane, co-clustering of K-RasG12V-S181 with K-RasG12V-S181D and with K-RasG12V-S181A was analyzed after phosphorylation induction (PMA+W13) or phosphorylation inhibition (BIM), using the immuno-EM-statistics approach indicated above (Fig. 3B,D).

Clustering of PI3K-p110α with phosphorylated K-Ras

To analyze the functional significance of the different clustering of oncogenic K-Ras according to its phosphorylation status, the above immuno-EM-statistics approach was used again. Cells were co-transfected with mGFP-p110α and mCherryK-RasG12V-S181D or mCherryK-RasG12V-S181A, and processed as indicated in the previous section. Ripley's bivariate K-function showed a strong co-clustering of mGFP-p110α with the phosphomimetic K-Ras mutant, while excluding distribution was observed with the non-phophorylatable K-Ras. Finally, co-clustering analysis of mGFP-p110α with phosphorylatable K-Ras after phosphorylation induction (PMA+W13) or inhibition (BIM), conclusively demonstrated that PI3K-p110α is efficiently recruited to the phosho-K-Ras segregated clusters (Fig 3C,D).

Through an integrated approach of density gradient fractionation and immuno-EM-statistics, we have found striking evidence of oncogenic K-Ras lateral segregation in the inner leaflet of plasma membrane by means of phosphorylation at Ser181 with a functional significance. We demonstrated that phosphorylated K-Ras exhibits a higher association with active c-Raf1 and PI3K (p110α), and at the nanoscale, it clusters together with PI3K (p110α). Since nanoclusters operate as temporary signaling platforms at the plasma membrane which contain certain mixtures of kinases,

phosphatases and other signaling proteins (Inder et al., 2008;Prior et al., 2003), molecular environment facilitating activation of major K-Ras effectors is expected to be found in the phospho-K-Ras platforms (Fig. 4). Our findings provide a novel rationale to explain how oncogenic K-Ras molecules, which are always GTP-loaded and thus presumably active, exhibit a differential signaling after phosphorylation.

MATERIALS AND METHODS

Cell culture

Human Epithelial Kidney cell lines (HEK293T) and HeLa cell lines were grown in Dulbecco's Modified Eagle's Medium (DMEM) containing 10% FBS (Biological Industries), pyruvic acid, antibiotics, and glutamine.

Antibodies and reagents

Primary antibodies: Anti-Raf-1 (#610152; BD Transduction Laboratories, San Jose, CA); Anti-phospho-Ser338-Raf-1 (#05534;Millipore, Billerica, MA, USA) ; Anti-PI3Kinase p110α (clone C73F8) (#4249; Cell Signalling, Danvers, MA, USA); Anti-HA (clone HA-7) (#A2095; Sigma, St. Louis, MO, USA); Anti-RFP rabbit (#A01388-40; GenScript, Piscataway, NJ, USA); Anti-GFP mouse (#ADI-SAB-500-E; Stressgene); Anti-K-Ras (Ab-1) (#OP24; Calbiochem); Anti-H-Ras (C-20) (#sc-520, Santa Cruz, Santa Cruz, CA, USA), Anti-Na^+/K^+-ATPase (clone C464.6) (#05-369X-555; Millipore); Anti-EEA1 (#610457; BD Bioscience, Franklin Lakes, NJ USA); Anti-Sec61α (#07-204; Millipore); Anti-Cav1 (#610407; BD Bioscience).

PMA (phorbol-12-myristate-13-acetate) and W13 (N-(4-aminobutyl)-5-cloro-2-naphtalensulphonamide) were from Sigma, (St. Louis, Mo, USA) and BIM (bisindolylmaleimide) From Calbiochem.

Immunoprecipitation

HeLa cells (1 x 100-cm dish) co-transfected with myc-Raf-1 and either HA-K-RasG12V-S181A or HA-K-RasG12V-S181D by X-tremeGENE HP DNA Transfection Reagent (Roche) were lysed in Ras extraction buffer (Alvarez-Moya et al. ,2010) and

the lysate incubated for 3h at 4ºC with HA-tag antibody crosslinked to Dynabeads, washed 3 times and eluted with glycine 200 mM pH2,5.

Confocal Microscopy

To determine mCherry-RasG12V-S181D and YFP-K-RasG12V-S181A colocalization, YFP and mCherry images were acquired sequentially using 514 and 561 laser lines, emission detection ranges 525-573 nm and 580-700 nm respectively and the confocal pinhole set at 1 Airy units. Images were acquired at 400 Hz in a 1024 x 1024 pixels format, zoom at 4 and pixel size of 60 x 60 nm.

FRET measurements were based on the acceptor photobleaching method and performed as previously decribed (Vila de la Muga et al. 2009).

Density gradient

HEK293T cells (7x150 cm dish plates) were transfected by Calcium Phosphate and after 24-48h cell membrane fractionation into a continuous OptiPrep density gradient was performed as previously described (Macdonald and Pike, 2005) with the exception of the densities used (sample at 20% and continuous gradient from 15% to 0% (v/v)) Gradients were fractionated into 670 µL fractions.,

High-resolution analysis of plasma membrane K-Ras clustering

HeLa cells were grown on coverslips at low density and co-transfected either with YFP- or mCherry- K-RasG12V, K-RasG12V-S181A, K-RasG12V-S181D; or with GFP-p110α and mCherry- K-RasG12V, K-RasG12V-S181A or K-RasG12V-S181D by GeneJuice (Merck Millipore) according to the manufacturer's specifications. After 24h of transfection cells were fixed in 4% paraformaldehyde plus 0.1% glutaraldehyde, and labeled with gradient-purified 2nm- and 5nm-conjugated antibodies, as previously described (Prior et al., 2003). Plasma membrane sheets were imaged using an FEI 120kV Tecnai transmission electron microscope obtaining images at 87,000 x magnification. Image processing and Bivariate K-Ripley Function analysis was performed to examine whether either gold particle population, at a distance r, is clustered around the other. Significance test of Bivariate K-Ripley Function were performed by Monte Carlo methods as described (Prior et al., 2003).

Acknowledgements

We are grateful to Dr. R Marais (UK Cancer Research Centre, London, England) for kindly providing the pEF-HA-K-RasG12V and Myc-Raf-1 plasmids, to Dr. J F Hancock (University of Texas, Houston, USA) for the pEGFP-p110α plasmid and to the advanced optical microscopy unit of CCiT-UB for technical assistance. This study was supported by MICINN-Spain [SAF2010-20712 and BFU2009-13526]. Carles Barceló is the recipient of the pre-doctoral fellowship "FPU" from MEC-Spain, Noelia Paco from the Catalan Governament, and Mariona Gelabert from MICINNSpain.

FIGURES LEGENDS

Fig 1. **Differential interaction of oncogenic K-Ras with phospho-Ser338- Raf-1 and catalytic subunit of PI3K according to K-Ras Ser181 phosphorylation status**. **(A)** HeLa cells co-expressing YFP-Raf-1 and Cer-K-RasG12V-S181A or Cer-K-RasG12V-S181D were measured using acceptor photobleaching FRET microscopy. Corrected FRET is presented as a quantitative pseudocolor image (right column); (**B**) The graph shows corrected FRET efficiency ± SEM from (A); **(C)** Cells as in (A) were stained with anti-phospho-Ser-338-Raf-1 and incubated with Alexa647-labeled secondary antibody. Corrected P-Raf-1 efficiency is presented as a quantitative pseudocolor image (right column); **(D)** Quantification of Raf-1 Ser338-phosphorylation efficiency (P-Raf-1/Raf-1) from (C); **(E)** HeLa cells were co-transfected with both myc-Raf-1 and either HA-K-RasG12V-S181A (non-phosphorylatable) or HA-K-RasG12V-S181D (phosphomimetic). Cell lysates were immunoprecipitated with anti-HA antibody or mouse IgG (IgG) and the input and the bound fractions were immunoblotted with the indicated antibodies. (***, $p<0.0001$, **$p<0.001$ and *$p<0.01$, p value for Student's two-tailed t test; ns: non-significant differences; mean and SEM are represented).

Fig 2. **Separation of oncogenic K-Ras according to its phosphorylation status into different density fractions**. **(A)** HEK 293 cells were co-transfected with the indicated pairs of K-Ras phosphomutants and localization analyzed by confocal microscopy. **(B,C,D,E)** HEK293 cells co-transfected with the indicated constructs were lysed in a detergent-free method and post-nuclear supernatant was fractionated into an Optiprep gradient fraction. **(B)** Phosphomutants and membrane markers distribution from HEK293 cells co-transfected with YFP-K-RasG12V-S181A/mCh-K-RasG12V-S181D was analyzed by western blotting. **(C)** Quantification of phosphomutants and endogenous K-Ras along the generated Optiprep gradient fractions from panel B (left). Distribution of both Optiprep and protein concentration (right). **(D)** A possible tag-effect was discarded by exchanging the tags of the phosphomutants (YFP-K-RasG12V-S181D/mCh-K-RasG12V-S181A) and performing the same fractionation as in **(B)**. **(E)** Partial overlapping of wild type-Ser181 mCh-K-RasG12V with phosphomimetic YFP-K-RasG12V-S181D

Fig 3. Spatial segregation of oncogenic K-Ras into functionaly different non-overlapping nanodomains according to Ser181 phosphorylation.. **(A)** HeLa cells were co-transfected with the pairs YFP-K-RasG12V-S181D/mCh-K-RasG12V-S181D to study a possible tag-effect when performing the analysis and with YFP-K-RasG12V-S181D/mCh-K-RasG12V-S181A to estimate clustering overlapping. **(B)** HeLa cells were co-transfected with the pairs YFP-K-RasG12V-S181D/mCh-K-RasG12V-S181 and after 24h of expression were either left untreated (control, blue line), serum starved for 6h and treated with 100 nM PMA + 15 µg/ml W13 for 30 min (to promote K-Ras phosphorylation, red line), or treated with 5µM BIM for 1h (to inhibit PKC, green line). (C) HeLa cells were co-transfected with the pairs mCh-K-RasG12V-S181D/EGFP-p110α or mCh-K-RasG12V-S181A/EGFP-p110α to estimate clustering overlapping (left panel). HeLa cells were co-transfected with mCh-K-RasG12V/EGFP-p110α and treated as in (B) to either promote (PMA+W13) or prevent (BIM) K-Ras phosphorylation. In (A), (B) and (C), CI means confidence interval (values above this line indicate co-clustering). (D) Examples of EM immunogold images used to perform analysis shown I (A), (B) and (C).

Fig 4. Model for the spatial segregation of oncogenic K-Ras by Ser181 phosphorylation. (A) Schematic representation of K-Ras structure showing the composition of the wildtype and phosphomutants C-terminal polybasic domains. Positively-charged residues (blue), negatively-charged (red), non-charged (black). (B) Image showing real localization of K-Ras molecules (from Fig. S2) and speculative distribution of active K-Ras effectors. Upon Ser181 phosphorylation, oncogenic K-Ras molecules migrate to spatially distinct non-raft nanodomains forming non-overlapping nanoclusters or, alternatively, phosphoryation is induced a preexisting nanocluster. Phospho-Ser181-K-RasG12V nanoclusters serves as preferential signaling platforms for the activation of main K-Ras effectors.

References

Abankwa, D., Gorfe, A. A. and Hancock, J. F. (2008). Mechanisms of ras membrane organization and signalling: Ras on a rocker. *Cell Cycle* **7,** 2667-2673.

Ahearn, I. M., Haigis, K., Bar-Sagi, D. and Philips, M. R. (2011). Regulating the regulator: Post-translational modification of RAS. *Nat. Rev. Mol. Cell Biol.* **13,** 39-51.

Alvarez-Moya, B., Barcelo, C., Tebar, F., Jaumot, M. and Agell, N. (2011). CaM interaction and Ser181 phosphorylation as new K-ras signaling modulators. *Small GTPases* **2,** 99-103.

Alvarez-Moya, B., Lopez-Alcala, C., Drosten, M., Bachs, O. and Agell, N. (2010). K-Ras4B phosphorylation at Ser181 is inhibited by calmodulin and modulates K-ras activity and function. *Oncogene* **29,** 5911-5922.

Ballester, R., Furth, M. E. and Rosen, O. M. (1987). Phorbol ester- and protein kinase C-mediated phosphorylation of the cellular kirsten ras gene product. *J. Biol. Chem.* **262,** 2688-2695.

Bivona, T. G., Quatela, S. E., Bodemann, B. O., Ahearn, I. M., Soskis, M. J., Mor, A., Miura, J., Wiener, H. H., Wright, L., Saba, S. G. et al. (2006). PKC regulates a farnesyl-electrostatic switch on K-ras that promotes its association with bcl-XL on mitochondria and induces apoptosis. *Mol. Cell* **21,** 481-493.

Fivaz, M. and Meyer, T. (2005). Reversible intracellular translocation of KRas but not HRas in hippocampal neurons regulated by Ca2+/calmodulin. *J. Cell Biol.* **170,** 429-441.

Hancock, J. F., Magee, A. I., Childs, J. E. and Marshall, C. J. (1989). All ras proteins are polyisoprenylated but only some are palmitoylated. *Cell* **57,** 1167-1177.

Hancock, J. F. and Parton, R. G. (2005). Ras plasma membrane signalling platforms. *Biochem. J.* **389,** 1-11.

Inder, K., Harding, A., Plowman, S. J., Philips, M. R., Parton, R. G. and Hancock, J. F. (2008). Activation of the MAPK module from different spatial locations generates distinct system outputs. *Mol. Biol. Cell* **19,** 4776-4784.

Kholodenko, B. N., Hancock, J. F. and Kolch, W. (2010). Signalling ballet in space and time. *Nat. Rev. Mol. Cell Biol.* **11,** 414-426.

Lopez-Alcala, C., Alvarez-Moya, B., Villalonga, P., Calvo, M., Bachs, O. and Agell, N. (2008). Identification of essential interacting elements in K-ras/calmodulin binding and its role in K-ras localization. *J. Biol. Chem.* **283,** 10621-10631.

Macdonald, J. L. and Pike, L. J. (2005). A simplified method for the preparation of detergent-free lipid rafts. *J. Lipid Res.* **46,** 1061-1067.

Plowman, S. J., Ariotti, N., Goodall, A., Parton, R. G. and Hancock, J. F. (2008). Electrostatic interactions positively regulate K-ras nanocluster formation and function. *Mol. Cell. Biol.* **28,** 4377-4385.

Plowman, S. J., Muncke, C., Parton, R. G. and Hancock, J. F. (2005). H-ras, K-ras, and inner plasma membrane raft proteins operate in nanoclusters with differential dependence on the actin cytoskeleton. *Proc. Natl. Acad. Sci. U. S. A.* **102,** 15500-15505.

Prior, I. A., Harding, A., Yan, J., Sluimer, J., Parton, R. G. and Hancock, J. F. (2001). GTP-dependent segregation of H-ras from lipid rafts is required for biological activity. *Nat. Cell Biol.* **3,** 368-375.

Prior, I. A., Lewis, P. D. and Mattos, C. (2012). A comprehensive survey of ras mutations in cancer. *Cancer Res.* **72,** 2457-2467.

Prior, I. A., Muncke, C., Parton, R. G. and Hancock, J. F. (2003). Direct visualization of ras proteins in spatially distinct cell surface microdomains. *J. Cell Biol.* **160,** 165-170.

Prior, I. A., Parton, R. G. and Hancock, J. F. (2003). Observing cell surface signaling domains using electron microscopy. *Sci. STKE* **. 177,** 9.

Schubbert, S., Shannon, K. and Bollag, G. (2007). Hyperactive ras in developmental disorders and cancer. *Nat. Rev. Cancer.* **7,** 295-308.

Silvius, J. R. (2002). Mechanisms of ras protein targeting in mammalian cells. *J. Membr. Biol.* **190,** 83-92.

Tian, T., Harding, A., Inder, K., Plowman, S., Parton, R. G. and Hancock, J. F. (2007). Plasma membrane nanoswitches generate high-fidelity ras signal transduction. *Nat. Cell Biol.* **9,** 905-914.

Vila de Muga, S., Timpson, P. Cubells, L., Evans R., Hayes, T.E., Rentero, C., Hegemann,A., Rverter, M., Leschner, J., Pol, A., Tebar, F., Daly, R.J., Enrich, C. and Grewal, T. (2009). Annexin A6 inhibits Ras signalling in breast cancer cells. *Oncogene* **28,** 363-377.

Yeung, T., Terebiznik, M., Yu, L., Silvius, J., Abidi, W. M., Philips, M., Levine, T., Kapus, A. and Grinstein, S. (2006). Receptor activation alters inner surface potential during phagocytosis. *Science* **313,** 347-351.

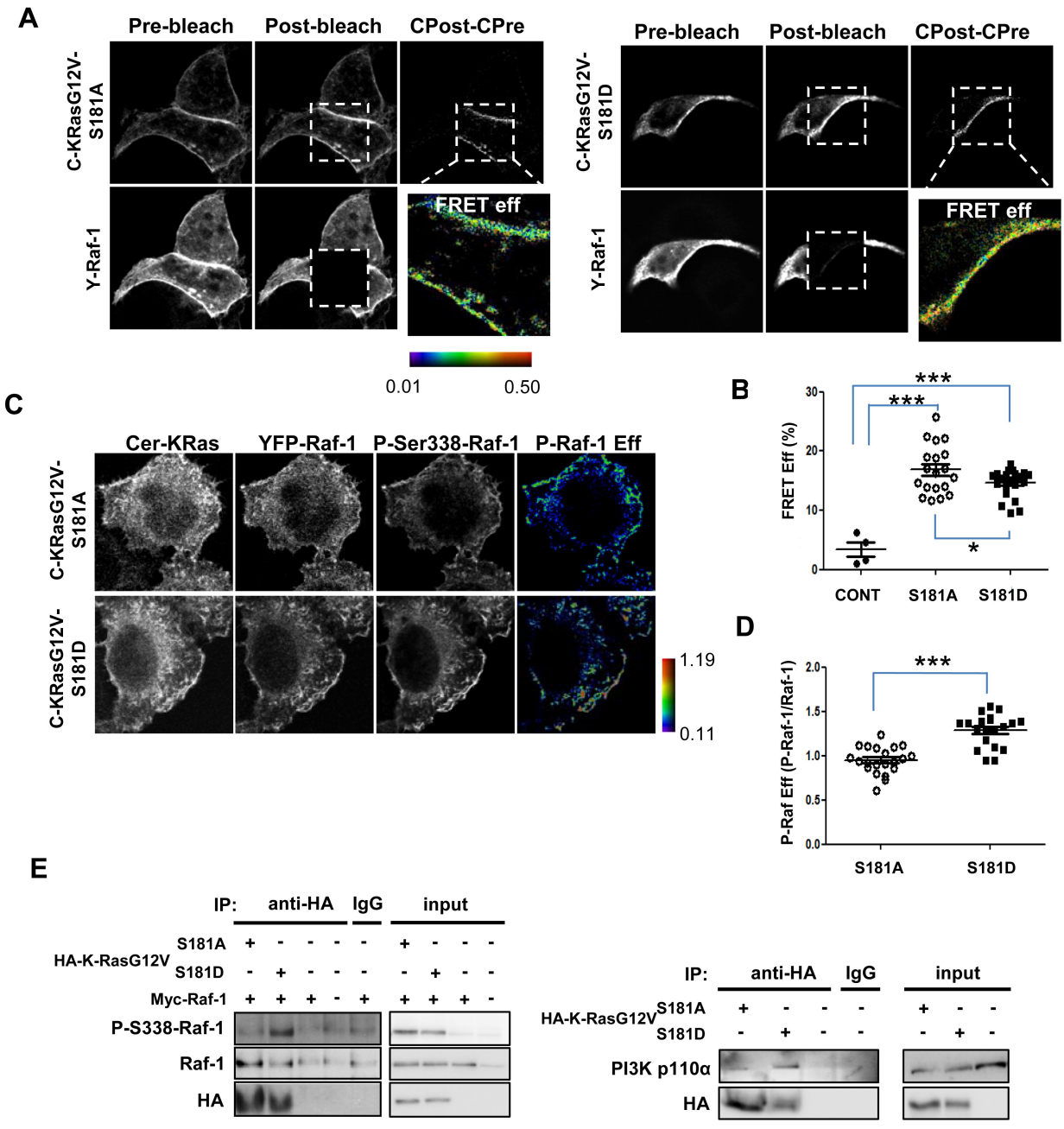

Fig 2